UNIVERSITY OF
BATH

University of Bath

Dual-function cellulose composites for fluorescence detection and removal of fluoride

Meng Li,[a] Zhijiang Liu,[a] Hui-Chen Wang, [b] Adam C. Sedgwick,[b] Jordan E. Gardiner,[b] Steven D. Bull, [b] Hui-Ning Xiao[a*] and Tony D. James[b*]

[a]Department of Environmental Science and Engineering, North China Electric Power University, Baoding, 071003, China. Email: hnxiao@ncepu.edu.cn

[b]Department of Chemistry, University of Bath, Bath, BA2 7AY, UK

Email:t.d.james@bath.ac.uk

Abstract: A biodegradable and robust fluorogenic cellulose material for simultaneous fluoride recognition and adsorption at environmentally significant levels is presented. The fluorescent modified cellulose (FMC) containing a boronic acid-based anthracene group as a fluorescent signaling unit displays a selective fluorescence enhancement with F^-. On the other hand, Cl^-, Br^-, SO_4^{2-}, $H_2PO_4^-$ and ClO_4^- did not induce significant changes in fluorescence. Furthermore, FMC shows excellent F^- adsorption over a wide range of pH with a low dosage. Equilibrium studies demonstrate that the adsorption of F^- follows the Langmuir model in an aqueous solution. While, adsorption kinetics were found to follow the pseudo-second-order model. The simplicity of the method and the ability to detect and remove fluoride in waste water is noteworthy given the problems associated with fluoride pollution in drinking water.

1. Introduction

Environmental pollution by fluoride anion is one of the main problems to be addressed in the treatment of drinking water. At low levels fluoride anions have been shown to be effective in the prevention of dental caries [1], however, high levels of fluoride in drinking water can cause both dental and skeletal fluorosis [2, 3]. Therefore, it is necessary to develop methods for highly selective and rapid detection and removal of fluoride ions. Various methods have been reported for the detection of fluoride such as fluoride electrodes [4, 5], gas chromatography (GC) [6], high pressure liquid chromatograph (HPLC) [7], and flow injection-spectrophotometry [8]. Among various sensors for detecting fluoride ion, fluorescence sensors have been widely investigated due to their high sensitivity, selectivity, and the potential for rapid real-time monitoring [9-14]. Sensors selective for fluoride have been designed *via* hydrogen bonding [15-19], anion–π interactions[20], and Lewis acid–based interactions [21-23]. In particular, those based on the affinity of a boron atom toward fluoride anion represent an attractive approach due to the excellent selectivity and sensitivity for fluoride anion with fluorescence "turn-on" [24-26]. The anthracene moiety is a particularly useful fluorophore used for the construction of fluorogenic chemosensors which have been employed for the detection of a variety of chemical species [27, 28]. Therefore, we decided to take advantage of these properties in the design of a fluoride specific sensor,

and prepared an anthracene appended boronic acid group **1** as a robust system for the detection of fluoride (Scheme 1).

Among the techniques used for the removal of fluoride anion from water, adsorption is one of the most effective and efficient methods [29, 30]. Biopolymer-based adsorbents have attracted significant attention as promising materials for the removal of fluoride ions, such as chitosan [31, 32] and cellulose [33, 34]. Cellulose is the most abundant polysaccharide and contains a number of hydroxyl groups which can be used for functional group modification in order to improve the chemical and physical properties [35-37]. Although cellulose based fluorescent sensors have been reported [38], there are few examples in the literature where the dual detection and adsorption properties of functional cellulose materials have been reported for the simultaneous sensing and removal of fluoride ions. Herein, we describe a novel fluorescent probe-modified cellulose material for the simultaneous fluoride ion detection and adsorption (Scheme 1). Such materials have huge potential in sensing and purification technologies, which also contributes to the development of sensing devices.

Insert Scheme 1

2. Experimental

2.1 Materials and equipment

All chemical reagents and solvents were analytical grade and purchased from commercial suppliers. Fluorescent modified cellulose was prepared by the established literature procedure [29].^{1}H NMR and ^{13}C NMR spectra were recorded on either a Bruker AV-300 or AV-250 spectrometer with chemical shifts reported in ppm (in $CDCl_3$,

TMS as internal standard) at room temperature. Electrospray mass spectra were recorded using a Bruker micro TOF spectrometer using reserpine as calibrant. FTIR spectra were recorded on the Nicolet iS-50 spectrometer at room temperature. SEM spectra were recorded using a JEOL JSM-7500F. Fluorescence measurements were performed on a Lengguang Luminescence spectrophotometer F97PRO (Shanghai), utilising sterna silica (quartz) cuvettes with 10 mm path length and four sides polished. Fluoride ion absorption experiments were employed by a Leici PXSJ-216F fluoride ion meter (Shanghai). Electric conductivity titration was recorded on a Shengci DDS-ⅡA conductivity meter (Shanghai). Spectral-grade solvents were used for measurements of fluoride absorption and fluorescence detection.

2.2 Synthesis

Insert Scheme 2

Synthesis of MonoBoctriamine (4)

Bis(hexamethylene)triamine (2.15 g, 10 mmol) was dissolved in MeOH (50 mL) then cooled in an ice bath. (Boc)$_2$O (0.436 g, 2 mmol) in MeOH (10 mL) was added slowly into the solution at 0 °C then the mixture was stirred continuously whilst warming from 0 °C to room temperature over 2 hours (monitoring by TLC). When the reaction finished, methanol was evaporated and water was added into the mixture. The pH of the mixture was adjusted to pH 7 (using 1 N NaOH and 1 N HCl) and extracted with DCM / water to remove the diboctriamine. Then the pH was adjusted to pH 10 with 1N NaOH and extracted with DCM to give the monoBoctriamine (0.543 g, 86%). ^{1}H NMR

(CD$_3$OD, 300 MHz, ppm) δ 1.37-1.48 (m, 21H), 1.64-1.65 (m, 4H), 2.85 (t, J= 6.0 Hz, 6H, -CH$_2$-N), 3.03 (t, J= 6.0 Hz, 2H, -CH$_2$-N-Boc). ^{13}C NMR (CD$_3$OD, 75 MHz, ppm) δ 27.6, 27.8, 27.9, 28.0, 28.5, 28.6, 29.3 (Boc-3CH$_3$), 30.1, 31.2, 41.5, 41.6, 49.9, 80.2, 159.0. ESI mass [M+H] C$_{17}$N$_{38}$N$_3$O$_2$ calculated 316.2964 found 316.2958.

tert-Buty(6-((6-((anthracen-9-ylmethyl)amino)hexyl)amino)hexyl)carbamate (3)

MonoBoctriamine (3.065 g, 9.7 mmol) and 9-anthracenecarboxaldehyde (1.8 g, 8.74 mmol) were dissolved in DCM / Methanol (1:1) (50 mL) and stirred overnight. After crude NMR confirmed that the imine had been generated, the reaction was cooled to room temperature. Sodium borohydride (3.67 g, 9.7 mmol) was added and stirred for another 2 hours. After the reaction was completed, more water (50 mL) was added to quench the unreacted NaBH$_4$. After evaporating methanol, the aqueous layer was extracted with DCM, dried with Na$_2$SO$_4$ and purified by flash column chromatography using DCM / MeOH as eluent to afford the product (3.67 g, 83%). ^{1}H NMR (CDCl$_3$, 250 MHz, ppm) δ 1.16-1.46 (m, 25H), 2.39-2.45 (m, 4H), 2.75 (t, J= 7.5 Hz, 2H), 2.93 (m, 2H), 4.56 (s, 2H), 7.30-7.45 (m, 4H), 7.85 (d, J= 7.5 Hz, 2H), 8.22-8.25 (m, 3H). ^{13}C NMR (CDCl3, 62 MHz, ppm) δ 26.5, 26.7, 27.0, 27.3, 27.7, 28.2, 28.4, 28.6, 30.0, 40.4, 45.7, 49.9, 50.0, 50.5, 78.5, 123.4, 124.9, 125.7, 126.2, 128.0, 130.2, 131.5, 131.8, 156.1. ESI mass [M+H] C$_{32}$H$_{48}$N$_3$O$_2$ calculated 506.3747 found 506.3708.

Synthesis of BOC protected anthracene based boronic acid sensor (2)

Tert-buty(6-((6-((anthracen-9-ylmethyl)amino)hexyl)amino)hexyl)carbamate (3.543 g, 7.01 mmol) was dissolved in dry THF (50 mL). Sodium hydride (0.616 g, 15 mmol,

60% in mineral oil) was slowly added into the solution and stirred for 20 mins, then 2-(bromomethyl)phenylboronic acid pinacol ester (4.45 g, 15 mmol) was added. The reaction was continuously stirred for 2 hours. After the reaction finished, the reaction mixture was quenched with water and poured into saturated $NaHCO_3$ solution (50 mL) to form the precipitate. The precipitate was then filtered, washed with water and hexane then dried to give the anthracene based boronic acid sensor (4.5 g, 83%). ^{1}HNMR (CDCl$_3$, 300 MHz, ppm) δ 1.30-1.35 (m, 25H), 2.48-2.50 (m, 6H), 3.03-3.05 (m, 2H), 4.02 (br, 4H), 4.47 (s, 2H), 7.21-7.51 (m, 10H), 7.75-7.83 (m, 2H), 7.91 (d, J= 8.4 Hz, 2H), 8.30 (s, 1H), 8.41 (d, J= 8.4 Hz, 2H).^{13}CNMR (CDCl$_3$, 75 MHz, ppm) δ 24.9, 25.0, 25.3, 26.5, 26.7, 27.0, 27.2, 28.5, 29.9, 40.5, 50.2, 53.8, 57.5, 74.9, 78.9, 83.6, 124.8, 125.3, 125.5, 126.0, 127.1, 128.8, 129.9, 130.0, 130.5, 131.2, 131.4, 131.5, 135.4, 146.3, 156.2. ESI mass [M-H_2O+H] $C_{46}H_{60}B_2N_3O_5$ calculated 756.4719 found 756.4736.

Synthesis of probe 1

Anthracene based boronic acid (0.10 g, 0.13 mmol) was dissolved in DCM and TFA (0.13 mmol, 9.67 μL) was added into the solution. The reaction was monitored by TLC and mass spectrometry, sometimes more TFA could be added if necessary. After the Boc protecting group was removed, all solvents were evaporated and extracted from DCM and 1 M NaOH to get probe **1** (quantitative yield). ESI mass [M-H_2O+H] $C_{41}H_{52}B_2N_3O_3$ calculated 656.4195 found 656.4300. NMR analysis of probe 1 was performed but the spectra we very broad and complex due to the formation of "oligomeric anhydrides" that complicated the "characterization efforts" [39]

Preparation for FMC fibre composites

Cotton lint fibre (18 g) was added into aqueous solution of sodium hydroxide (500 mL,15%,w/v). The resulting mixture was stirred for 2h and kept at 60℃. The resulted suspension was washed thoroughly with deionized water and neutralized with HCl. The mixture of as-pretreated cellulose (2.5 g), TEMPO (2,2,6,6-tetramethylpiperidine-1-oxyl radical) (0.04 g)，NaBr (0.25 g) and Na_2CO_3/ $NaHCO_3$ buffer (pH=10.8, 100 mL) were stirred at 600 rpm while aqueous solution of sodium hydroxide (0.5 mol L^{-1}) was added to keep the pH at 10-11. Ethanol was also added to keep the pH constant.

The resulting suspension was centrifuged (10000 r/min, 15 min), washed with deionized water and ethanol. The precipitate was dried in vacuum oven (40 ℃) for 24h. Next, the resulted TEMPO oxidized cellulose was added to aqueous solution of sodium chlorite (200 mL,15% ,w/v, pH=4.8). After reaction for 3 hours, the mixture was centrifuged, washed and dried to afford final TEMPO oxidized cellulose (TOC). TOC (1.5 g) was dissolved in water (400 mL), and then EDC (0.51g, 2.67 mmol) and NHS (0.33g, 2.86 mmol) were added to the mixture. The pH of the resulting mixture was adjusted to 7.5-8 by aqueous solution of NaOH and HCl. The reaction was kept at r.t. until deionized water was added to remove redundant EDC/NHS and side products. Probe **1** (2 equiv. of COOH on TOC) was added and reacted with the mixture at r.t. for 24 h. When the reaction was completed, excess probe **1** was washed off. The final products were centrifuged and freeze-dried.

2.3 Fluorescence measurements

A stock solution of FMC (0.1 g L^{-1}) was prepared in MeOH-H_2O (4:1, v/v). A stock

solution of NaF was prepared in the same solvent system. Different concentrations of NaF were added into the solution. The stock solutions (10 mM) of various anions, such as Br^-, Cl^-, $H_2PO_4^-$, SO_4^{2-}, and ClO_4^-, were prepared using their sodium salts in MeOH-H_2O (4:1, v/v).

2.4 Adsorption measurements

For the adsorption experiments, NaF were used in this study. 5 mg FMC was added into 20 mL of fluoride anion solution for 30 mins except for the study of contact time. The amount of F^- in the solution was traced by a Leici PXSJ-216F fluoride ion meter (Shanghai).

The effect of contact time (0 to 30 min) and pH (2 to 12) were also investigated with 0.25 g L^{-1} of dry FMC and metals initial concentration of 10 mg L^{-1} and 5 mg L^{-1}, respectively. The adsorbed amounts of fluoride ions (Q_t, mg L^{-1}) were determined according to the Eq (1):

$$Q_t = \frac{(C_0 - C_t)*V}{W} \qquad (1)$$

Where C_0 is the initial solution concentration (mg L^{-1}), and C_t is the solution concentration at time t, V is the volume of solution (L) and W is the weight of dry FMC (g).

2.5 Recyclability

The recyclability of FMC was recorded at 25 °C 5 mg of FMC was added into 20 mL of 5 mg L^{-1} F^- solutions for 15 min. Then FMC was taken out from the solutions. The desorption and regeneration of the FMC adsorbed by fluoride ions were performed by

immersing FMC into 100 mL of 1.0 mol L^{-1} HNO_3 solution under agitating at 25 °C for 100 min and washed with DI water. The generated FMC were used for another adsorption in the subsequent cycles.

3. Results and discussion

3.1 Synthesis

Probe **1** was prepared by treatment of the BOC protected anthracene based boronic acid sensor with trifluoroacetic acid at room temperature for 5 hours in acetonitrile, followed by extraction from DCM and 1M NaOH, which resulted in the removal of the protecting group and afforded probe **1**. Cotton lint cellulose fibre was chosen as the base materials. After pretreatment and TEMPO (2,2,6,6-tetramethylpiperidine-1-oxyl radical) oxidation [40], the amine group (-NH_2) of probe **1** was reacted with the carboxyl group (-COOH) of the oxidized cellulose, using EDC as a coupling agent in the presence of an activation agent *N*-hydroxysuccinimide (NHS) [41]. Experimental details can be found in the Electronic Supplementary Information. The fluorescent-modified cellulose (FMC) was fully characterized by FTIR (Figure S2†) and SEM-EDS (Figure 2). In addition, the degree of the TEMPO oxidisation of cellulose was evaluated by an electric conductivity titration method (Figure S1). The COOH content was calculated to be 1.27 mmol g^{-1}. The FTIR spectra indicated a peak at 1564 cm^{-1} due to the -NH group in probe **1** modified cellulose, indicating the successful grafting of probe **1** onto the cellulose.

Figure 1 shows typical SEM images of the four-types of cellulose fibres. It was observed that the cellulose fibers loosen and become separated into individual fibers in the case of cellulose after chemical treatment. Figure 1b indicates that the oxidation reaction breaks up some of the cellulose fibres into smaller fibre fragments. The fibres get even smaller after modification with probe **1**. The coupling facilitated by EDC/NHS was confirmed by a high N content, 7.85 wt%, as revealed by the EDS of FMC (Figure 2).

Insert Figure 1 and Figure 2

3.2 Spectral studies of FMC

To gain an insight into the fluoride ion sensing of FMC, the emission at 417 nm was monitored with added fluoride anion. An increase in the fluorescence intensity of the anthracene emissions at 399 nm, 417 nm and 442 nm was observed. The fluoride anion concentration dependence of the relative fluorescence intensities at 417 nm is shown in Figure 3. We ascribe the increase in fluorescence to enhanced basicity of the nitrogen atoms proximal to the boronate anions formed on fluoride binding (*i.e.* it is easier to protonate the nitrogen when next an anionic boronate).

Insert Figure 3

Fluorescence titration of FMC with other anions was carried out in order to determine the selectivity (Figure S4). From these titrations it is clear that only the addition of

fluoride ions enhance the intensity of the fluorescence, while other anions only show subtle changes of the anthracene emission. From these observations it is clear that FMC exhibits high selectivity for fluoride anions over the other anions employed in this study.

Subsequently, fluoride ion adsorption was investigated in order to identify the optimal conditions for the maximum removal from aqueous solution. The effect of the initial concentration of F^- on the adsorption capacity is presented in Figure 4. The adsorption capacity of fluoride ion increased initially from 1.4 to 8.1 mg g^{-1} with the increasing F^- concentration (0−10 mg L^{-1}), and then reached equilibrium; whereas the adsorption rate decreased with an increase of F^- concentration, suggesting that the FMC is a very effective material for F^- adsorption at low concentrations.

Insert Figure 4

Based on a set of data related to the adsorption capacity at equilibrium (Q_e) and the equilibrium concentration of F^- in aqueous solution, both the Langmuir isotherm model and Freundlich model were fitted. The model fitting curves for F^- adsorption onto the FMC are shown in Figure S5 and S6. And the results are summarized in Table 1. The correlation coefficient for the Langmuir isotherm model is higher than that of the Freundlich isotherm model, indicating that Langmuir isotherm model matches the isothermal adsorption process of FMC better; and the F^- adsorbed onto the FMC was dominated by a monolayer adsorption process.

Insert Table 1

In batch experiments with 10 mg L^{-1} F^- at pH 6 and 30 °C adsorption was evaluated over 0 to 30 min. Adsorption capacity (Q) was observed to increase with time, and equilibrium was attained after 10 min with a maximum adsorption rate of 20% and maximum adsorption capacity of 7.5 mg g^{-1} (Figure 5). Based on these results, the adsorption kinetics models including the pseudo-first-order kinetic model and the pseudo-second-order kinetic model were explored. Both kinetic model curves fitted for F^- adsorption onto FMC are shown in Figure S7 and Figure S8. Clearly, the pseudo-second order kinetic model fits the experimental data with a correlation coefficient value ($R^2 = 0.998$) close to 1, when compared to the pseudo-first-order model ($R^2 = 0.957$), indicating that the pseudo-second order kinetic model better describes the kinetics of F^- ion adsorption onto FMC (Table 2). The adsorption mechanism is simultaneous physical adsorption and chemical adsorption.

Insert Figure 5 and Table 2

The effect of pH on the adsorption of F^- was investigated over the pH range of 2.0-12.0. As shown in Figure S9, adsorption displayed only subtle changes with an increase in pH. Therefore, FMC could be used for fluoride removal over a wide pH range.

The recyclability of FMC and the adsorption rate of fluoride ions are important in environmental protection (Figure S10). The regeneration of FMC was performed by

immersing the adsorbent into HNO_3 solution for 100 min. After five desorption cycles, the recyclable adsorption behavior of FMC toward F^- was similar and the adsorption rates were only slightly decreased. The removal efficiency of GMC toward F^- after one and five cycles was 30% and 26.0%, respectively. The excellent reusability indicates that FMC could be a potential absorbent in practical applications.

Evidence to support the adsorption of F^- was also obtained from the FTIR spectrum of the F-loaded FMC. The adsorption of F^- onto the polymer is indicated by the shifting of the position with the change in intensity of some basic peaks (Figure S2). The shift in the characteristic peak of $-OH$ from 1155 to 1164 cm^{-1} indicates that the $-OH$ group is the main adsorption site for F^- adsorption, which ascribes to intermolecular hydrogen bonding. Similarly, the SEM image of F-loaded FMC (Figure 1d) has different surface morphologies from its precursor FMC (Figure 1c). Furthermore, the EDS result of F-loaded FMC indicated the presence of a peak corresponding to F in the spectrum (Figure 2c), supporting the adsorption of fluoride ions onto the material.

4. Conclusion

A fluorogenic cellulose material was designed and evaluated to be an effective sensor and adsorbent for fluoride ion removal from aqueous solution. Fluoride ion sensing was investigated at a lower limit of 10 $mg\,L^{-1}$, and the adsorption was found to reach the plateau after 10 mins. The adsorption follows Langmuir isotherm and pseudo-second-order kinetics. We believe that these simple and robust materials represent excellent candidates for the simultaneous fluoride ion detection and removal from water in

purification technologies. Since there is a wide selection of fluorophores to facilitate the fabrication of fluorescent sensors with the desired sensing and removal performance, the strategy will enrich this research field and provide a new method for wide anion sensing and removal applications.

Acknowledgments

References

[1] Featherstone JD. Prevention and reversal of dental caries: role of low level fluoride. Community Dent Oral. 1999;27(1):31-40.

[2] Schwarzenbach RP, Escher BI, Fenner K, Hofstetter TB, Johnson CA, Von Gunten U, et al. The challenge of micropollutants in aquatic systems. Science. 2006;313(5790):1072-7.

[3] Ayoob S, Gupta AK. Fluoride in drinking water: a review on the status and stress effects. Crit Rev Env Sci Tec. 2006;36(6):433-87.

[4] Çiftçi H, Oztekin Y, Tamer U, Ramanavicine A, Ramanavicius A. Development of poly (3-aminophenylboronic acid) modified graphite rod electrode suitable for fluoride determination. Talanta. 2014;126:202-7.

[5] Un UT, Koparal AS, Ogutveren UB. Fluoride removal from water and wastewater with a bach cylindrical electrode using electrocoagulation. Chem Eng J. 2013;223:110-5.

[6] Chiba K, Yoshida K, Tanabe K, Ozaki M, Haraguchi H, Winefordner J, et al. Determination of ultratrace levels of fluorine in water and urine samples by a gas chromatographic/atmospheric pressure helium microwave induced plasma emission spectrometric system. Anal Chem. 1982;54(4):761-4.

[7] Musijowski J, Szostek B, Koc M, Trojanowicz M. Determination of fluoride as fluorosilane derivative using reversed‐phase HPLC with UV detection for determination of total organic fluorine. J Sep Sci. 2010;33(17‐18):2636-44.

[8] Themelis DG, Tzanavaras PD. Simultaneous spectrophotometric determination of

fluoride and monofluorophosphate ions in toothpastes using a reversed flow injection manifold. Anal Chim Acta. 2001;429(1):111-6.

[9] Li M, Guo Z, Zhu W, Marken F, James TD. A redox-activated fluorescence switch based on a ferrocene–fluorophore–boronic ester conjugate. Chem Commun. 2015;51(7):1293-6.

[10] Galbraith E, James TD. Boron based anion receptors as sensors. Chem Soc Rev. 2010;39(10):3831-42.

[11] Zhang X, Li H, Mu H, Liu Y, Guan Y, Yoon J, et al. Cholesteryl naphthalimide-based gelators: Their applications in the multiply visual sensing of CO_2 based on an anion-induced strategy. Dyes Pigments. 2017;147:40-9.

[12] Zhang S, Fan J, Zhang S, Wang J, Wang X, Du J, et al. Lighting up fluoride ions in cellular mitochondria using a highly selective and sensitive fluorescent probe. Chem Commun. 2014;50(90):14021-4.

[13] Peng X, Wu Y, Fan J, Tian M, Han K. Colorimetric and ratiometric fluorescence sensing of fluoride: tuning selectivity in proton transfer. J Org Chem. 2005;70(25):10524-31.

[14] Turan IS, Akkaya EU. Chemiluminescence sensing of fluoride ions using a self-immolative amplifier. Org Lett. 2014;16(6):1680-3.

[15] Ashokkumar P, Weißhoff H, Kraus W, Rurack K. Test‐Strip‐Based Fluorometric Detection of Fluoride in Aqueous Media with a BODIPY‐Linked Hydrogen‐Bonding Receptor. Angew Chem Int Edit. 2014;53(8):2225-9.

[16] Cho EJ, Moon JW, Ko SW, Lee JY, Kim SK, Yoon J, et al. A new fluoride selective

fluorescent as well as chromogenic chemosensor containing a naphthalene urea derivative. J Am Chem Soc. 2003;125(41):12376-7.

[17] Chen X, Leng T, Wang C, Shen Y, Zhu W. A highly selective naked-eye and fluorescent probe for fluoride ion based on 1, 8-naphalimide and benzothizazole. Dyes Pigments. 2017;141:299-305.

[18] Elmes RB, Gunnlaugsson T. Luminescence anion sensing via modulation of MLCT emission from a naphthalimide–Ru (II)–polypyridyl complex. Tetrahedron Lett. 2010;51(31):4082-7.

[19] Elmes RB, Turner P, Jolliffe KA. Colorimetric and luminescent sensors for chloride: hydrogen bonding vs deprotonation. Org Lett. 2013;15(22):5638-41.

[20] Guha S, Saha S. Fluoride ion sensing by an anion− π interaction. J Am Chem Soc. 2010;132(50):17674-7.

[21] Wu X, Chen X-X, Song B-N, Huang Y-J, Ouyang W-J, Li Z, et al. Direct sensing of fluoride in aqueous solutions using a boronic acid based sensor. Chem Commun. 2014;50(90):13987-9.

[22] Ke I-S, Myahkostupov M, Castellano FN, Gabbaï FoP. Stibonium ions for the fluorescence turn-on sensing of F–in drinking water at parts per million concentrations. J Am Chem Soc. 2012;134(37):15309-11.

[23] Hou P, Chen S, Wang H, Wang J, Voitchovsky K, Song X. An aqueous red emitting fluorescent fluoride sensing probe exhibiting a large Stokes shift and its application in cell imaging. Chem Commun. 2014;50(3):320-2.

[24] Nishimura T, Xu SY, Jiang YB, Fossey JS, Sakurai K, Bull SD, et al. A simple

visual sensor with the potential for determining the concentration of fluoride in water at environmentally significant levels. Chem Commun. 2013;49(5):478-80.

[25] Xu Z, Kim SK, Han SJ, Lee C, Kociok‑Kohn G, James TD, et al. Ratiometric fluorescence sensing of fluoride ions by an asymmetric bidentate receptor containing a boronic acid and imidazolium group. Eur J Org Chem. 2009;2009(18):3058-65.

[26] López-Alled CM, Sanchez-Fernandez A, Edler KJ, Sedgwick AC, Bull SD, McMullin CL, et al. Azulene–boronate esters: colorimetric indicators for fluoride in drinking water. Chem Commun. 2017, DOI: doi:10.1039/c7cc07416f.

[27] Shellaiah M, Wu Y-H, Singh A, Raju MVR, Lin H-C. Novel pyrene-and anthracene-based Schiff base derivatives as Cu^{2+} and Fe^{3+} fluorescence turn-on sensors and for aggregation induced emissions. J Mater Chem A. 2013;1(4):1310-8.

[28] Lu H, Xu B, Dong Y, Chen F, Li Y, Li Z, et al. Novel fluorescent pH sensors and a biological probe based on anthracene derivatives with aggregation-induced emission characteristics. Langmuir. 2010;26(9):6838-44.

[29] Bhatnagar A, Kumar E, Sillanpää M. Fluoride removal from water by adsorption— a review. Chem Eng J. 2011;171(3):811-40.

[30] Barathi M, Kumar ASK, Kumar CU, Rajesh N. Graphene oxide‑aluminium oxyhydroxide interaction and its application for the effective adsorption of fluoride. RSC Adv. 2014;4(96):53711-21.

[31] Viswanathan N, Meenakshi S. Development of chitosan supported zirconium (IV) tungstophosphate composite for fluoride removal. J Hazard Mater. 2010;176(1):459-65.

[32] Ma J, Shen Y, Shen C, Wen Y, Liu W. Al-doping chitosan–Fe (III) hydrogel for the

removal of fluoride from aqueous solutions. Chem Eng J. 2014;248:98-106.

[33] Tian Y, Wu M, Liu R, Wang D, Lin X, Liu W, et al. Modified native cellulose fibers—A novel efficient adsorbent for both fluoride and arsenic. J Hazard Mater. 2011;185(1):93-100.

[34] Yu X, Tong S, Ge M, Zuo J. Removal of fluoride from drinking water by cellulose@ hydroxyapatite nanocomposites. Carbohydr Polym. 2013;92(1):269-75.

[35] Kumari S, Chauhan GS. New Cellulose–Lysine Schiff-Base-Based Sensor–Adsorbent for Mercury Ions. ACS Appl Mater Inter. 2014;6(8):5908-17.

[36] Luo Y, Tang D, Zhu W, Xu Y, Qian X. Reactive fluorescent dye functionalized cotton fabric as a "Magic Cloth" for selective sensing and reversible separation of Cd^{2+} in water. J Mater Chem C. 2015;3(33):8485-9.

[37] Li M, Liu Z, Wang L, James TD, Xiao H-N, Zhu W-H. A glutamic acid-modified cellulose fibrous composite used for the adsorption of heavy metal ions from single and binary solutions. Mater Chem Front. 2017; 1: 2317-2323.

[38] Li M, Li X, Xiao HN, James T. Fluorescence Sensing with Cellulose‐Based Materials. ChemistryOpen, DOI: 10.1002/open.201700133.

[39] G. Dennis, Boronic acids: preparation and applications in organic synthesis, medicine and materials, Wiley, 2011.

[40] Isogai A, Saito T, Fukuzumi H. TEMPO-oxidized cellulose nanofibers. Nanoscale. 2011;3(1):71-85.

[41] Barazzouk S, Daneault C. Spectroscopic characterization of oxidized nanocellulose grafted with fluorescent amino acids. Cellulose. 2011;18(3):643-53.

Scheme Title and Captions of Figures

Scheme 1. Fluorescently Modified Cellulose (FMC) prepared using probe **1**.

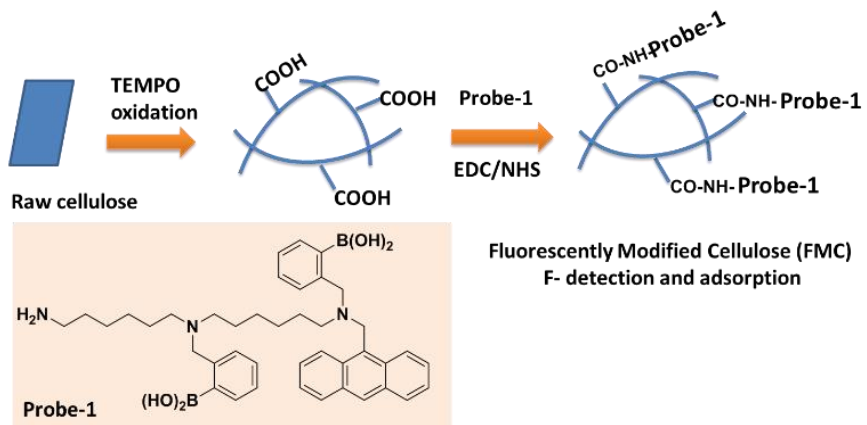**Scheme 2.** Synthetic route for **probe 1**

Figure 1. SEM images of a) pre-treated cellulose; b) TEMPO oxidised cellulose; c) FMC, and d) F-loaded FMC.

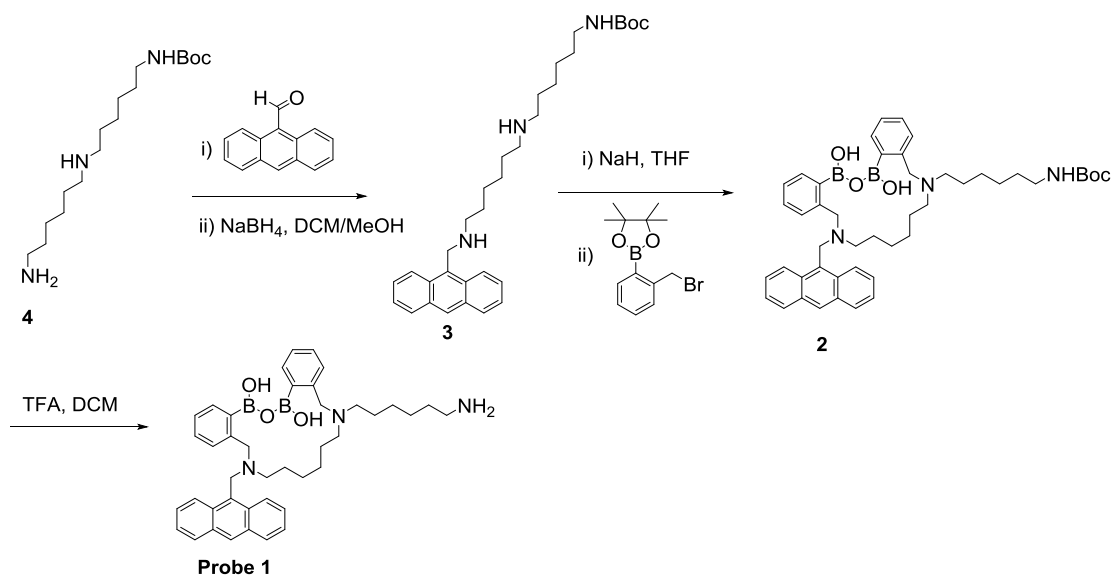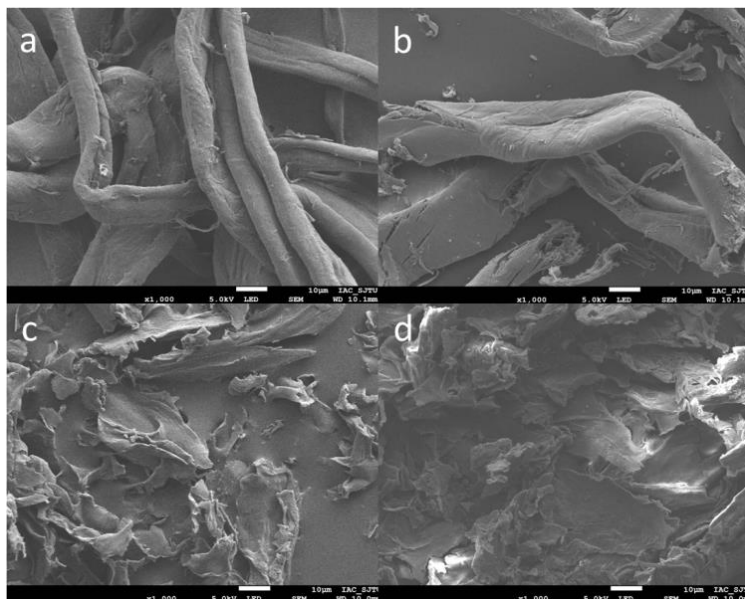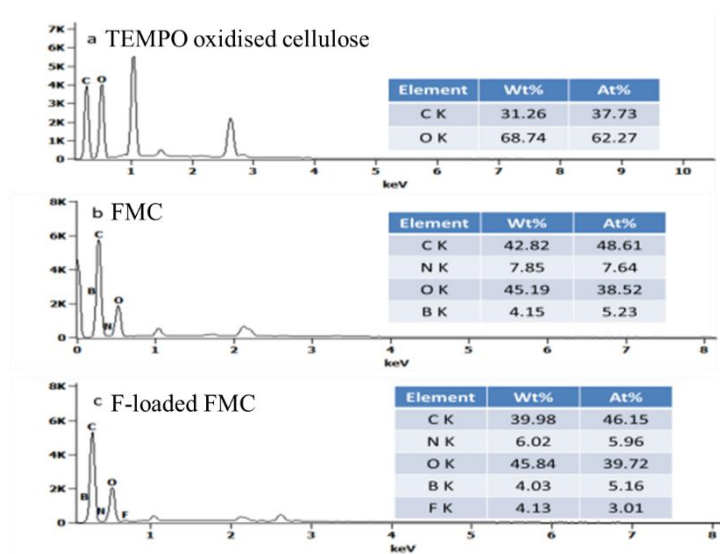**Figure 2.** EDS of a) TEMPO oxidised cellulose; b) FMC, and c) F-loaded FMC.

Figure 3. The relative fluorescence intensity at 417 nm plotted against fluoride anion concentration ([FMC]= 0.1 g L^{-1}; λ_{ex}= 280 nm).

Figure 4. Effect of F$^-$ initial concentration on adsorption rate and capacity ([FMC]=0.25 g L^{-1}, pH=6)

Figure 5 Effect of time on adsorption rate and capacity ([FMC]=0.25 g L^{-1}; [F$^-$]=10 mg L^{-1}, pH=6)

Scheme 1. Fluorescently Modified Cellulose (FMC) prepared using probe **1**.

Scheme 2. Synthetic route for **probe 1**

Figure 1. SEM images of a) pre-treated cellulose; b) TEMPO oxidised cellulose; c) FMC, and d) F-loaded FMC.

Figure 2. EDS of a) TEMPO oxidised cellulose; b) FMC, and c) F-loaded FMC.
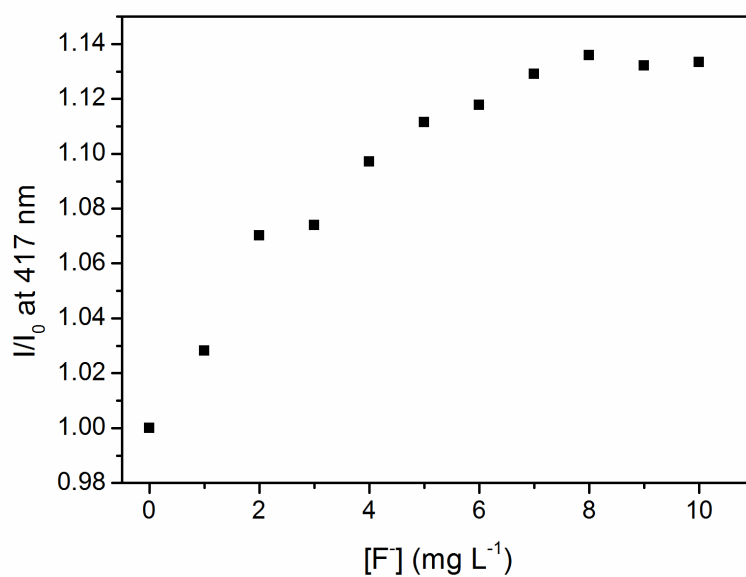
Figure 3. The relative fluorescence intensity at 417 nm plotted against fluoride anion concentration ([FMC]= 0.1 g L^{-1}; λ_{ex}= 280 nm).

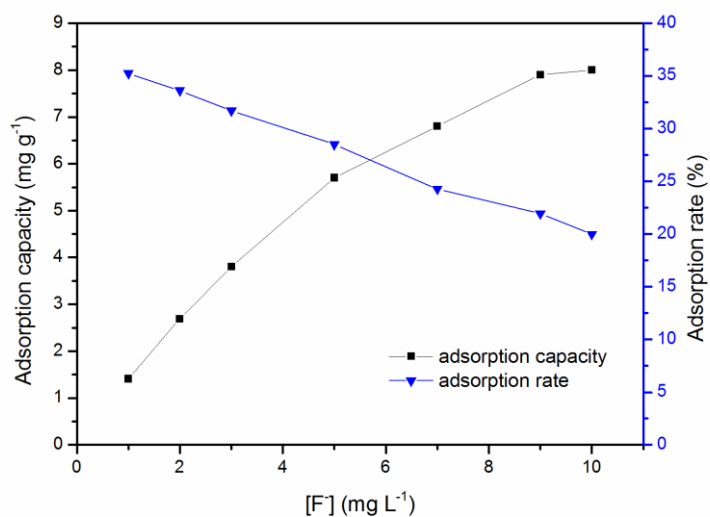**Figure 4.** Effect of F^{-} initial concentration on adsorption rate and capacity ([FMC]=0.25 g L^{-1} , pH=6)

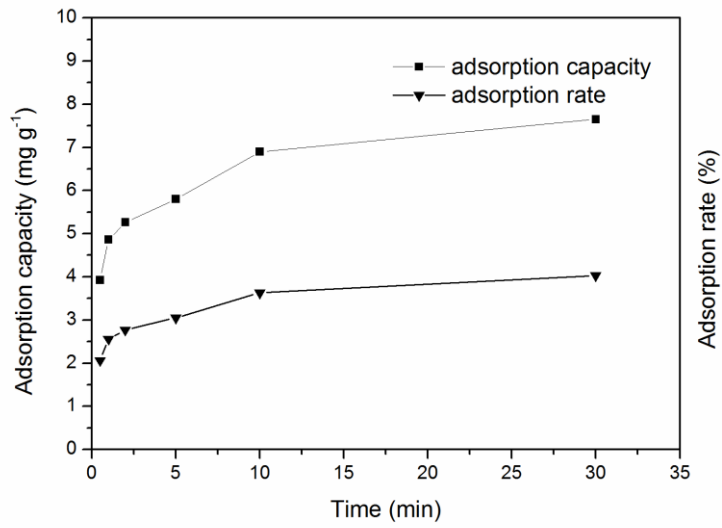**Figure 5.** Effect of time on adsorption rate and capacity ([FMC]=0.25 g L^{-1}; [F$^-$]=10 mg L^{-1}, pH=6)

Table 1. Langmuir and Freundlich parameters for F$^-$ adsorption

	Isotherm adsorption equations	k	R^2
Langmuir	C$_e$/Q$_e$=0.072C$_e$+0.393	0.184	0.9913
Freundlich	lnQ$_e$=0.689lnC$_e$+0.754	5.68	0.9780

Table 2. Kinetic parameters of F$^-$ absorption under different time duration

	Equations of kinetic	k	R^2
First-order	Ln(Q$_e$-Q)=-0.355t+1.9276	0.355	0.9574
Second-order	t/Q=0.1275+0.1274t	0.127	0.9977